



UNIVERSITY OF LEEDS

This is a repository copy of *Organic matter enrichment mechanism in saline lacustrine basins: A review*.

White Rose Research Online URL for this paper:

<https://eprints.whiterose.ac.uk/202338/>

Version: Accepted Version

---

**Article:**

Xu, S., Wang, Y. [orcid.org/0000-0001-9266-1778](https://orcid.org/0000-0001-9266-1778), Bai, N. et al. (2 more authors) (2024) Organic matter enrichment mechanism in saline lacustrine basins: A review. *Geological Journal*, 59 (1). pp. 155-168. ISSN 0072-1050

<https://doi.org/10.1002/gj.4853>

---

**Reuse**

Items deposited in White Rose Research Online are protected by copyright, with all rights reserved unless indicated otherwise. They may be downloaded and/or printed for private study, or other acts as permitted by national copyright laws. The publisher or other rights holders may allow further reproduction and re-use of the full text version. This is indicated by the licence information on the White Rose Research Online record for the item.

**Takedown**

If you consider content in White Rose Research Online to be in breach of UK law, please notify us by emailing [eprints@whiterose.ac.uk](mailto:eprints@whiterose.ac.uk) including the URL of the record and the reason for the withdrawal request.



[eprints@whiterose.ac.uk](mailto:eprints@whiterose.ac.uk)  
<https://eprints.whiterose.ac.uk/>

# 1           **Organic matter enrichment mechanism in saline** 2                           **lacustrine basins: A review**

3           Shang Xu <sup>1\*</sup> Yuxuan Wang <sup>2\*</sup>, Nan Bai <sup>3</sup> Shiqiang Wu <sup>4</sup> Bingchang Liu <sup>1</sup>

4                   <sup>1</sup> Shandong Provincial Key Laboratory of Deep Oil & Gas, China University of  
5    Petroleum, Qingdao 266580, China

6                   <sup>2</sup> Key Laboratory of Tectonics and Petroleum Resources, Ministry of Education,  
7    China University of Geosciences, Wuhan 430074, China

8                   <sup>3</sup> Zhanjiang Branch of CNOOC (China) Co., Ltd, Zhanjiang 524000, China

9                   <sup>4</sup> Research Institute of Petroleum Exploration & Development, SINOPEC  
10    Jiangnan Oilfield, Wuhan 430074, China

11           Correspondence:

12           **Shang Xu**, School of Geosciences, China University of Petroleum, Changjiangxi Road  
13           No.66, Qingdao 266580, China. E-mail: xushang0222@163.com.

14           **Yuxuan Wang**, Key Laboratory of Tectonics and Petroleum Resources, Ministry of  
15           Education, China University of Geosciences, Wuhan 430074, China. E-mail:  
16           wyx\_cug@163.com.

## 17           **Abstract**

18           Organic-rich shale in saline lacustrine basins holds significant importance as a  
19           source rock for conventional hydrocarbon exploration and has emerged as a prominent  
20           target for unconventional hydrocarbon exploration and development in recent years.  
21           Based on in saline lacustrine basins, this paper provides a summary of the organic

22 matter enrichment mechanisms in saline lacustrine basins, considering sedimentary  
23 characteristics, biological activities, factors for the organic matter enrichment and  
24 consumption, and hydrocarbon generation. The implications for these factors are  
25 discussed in relation to the distribution prediction of high-quality lacustrine shale  
26 district settings and the exploration and development of shale oil. Saline lacustrine  
27 basins undergo distinct evolutionary stages, each corresponding to different  
28 sedimentary stages involving carbonate minerals, sulfate minerals, and alkaline  
29 minerals. Moreover, these basins exhibit diverse biological types and experience  
30 extensive biological activities. The prosperity of organisms and the accumulation of  
31 sedimentary organic matter are ensured by halophilic organisms. Organic matter  
32 enrichment in saline lacustrine basins is influenced by two main aspects: the primary  
33 productivity of organic matter, which is promoted by the proliferation of halophilic  
34 organisms, and the efficient preservation of organic matter facilitated by the strong  
35 reducing environment resulting from promoted water salinity stratification. The organic  
36 matter consumption in saline lacustrine basins involves bacterial sulfate reduction (BSR)  
37 in the early stages, thermochemical sulfate reduction (TSR) in the late stages, and  
38 dilution of salt minerals with higher depositional rates. of the presence of salt beds and  
39 saline minerals positively influences hydrocarbon generation and expulsion in organic-  
40 rich shale within saline lacustrine deposition. Consequently, continental saline  
41 lacustrine basins in China offer favorable conditions for the formation of organic-rich  
42 shale and present broad prospects for for the exploration of shale oil and gas resources.

## 43 **Keywords**

44 Biological activities, Consumption of organic matter, Enrichment of organic matter,  
45 Saline lacustrine basins, Shale oil

## 46 **1 INTRODUCTION**

47 Source rocks associated with evaporation and saltwater are widely distributed  
48 globally, encompassing numerous renowned marine and continental basins (Warren,  
49 2016; Figure 1). Those organic-rich shales, that formed under a saline backdrop, serve  
50 as crucial source rocks for conventional and unconventional hydrocarbon exploration  
51 and development in recent years (Jin et al., 2006). A saline lacustrine basin is  
52 characterized by a lake basin with salinity levels exceeding 1‰, typically resulting from  
53 a higher rate of water evaporation compared to water influx (Jiang et al., 2004). The  
54 presence of Ca-Mg carbonate minerals often marks the initiation of a saline lacustrine  
55 basin. With the increasing lake water salinity, minerals such as sodium carbonate,  
56 sulfate, and chloride are also deposited. From the Permian to the Paleogene periods,  
57 there are numerous saline lacustrine basins and strata developed in China (Figure 2). In  
58 the 1980s, the interbedding of evaporites and source rocks was discovered in the  
59 Jiangnan Basin, while the Dongpu Depression of Bohai Bay Basin revealed the  
60 coexistence of extensive salt rocks and shale (Jiang, Sheng, & Fu, 1988; Jin & Huang,  
61 1985). In recent years, significant advancements have been made in the exploring and  
62 developing the continental shale oil in China, shedding light on the mixed deposition  
63 and interbedded relationships between high-quality shale and salt minerals (Zhi et al.,

64 2016, Zeng et al., 2017). This indicates the crucial role of saline lacustrine basins in the  
65 formation of organic-rich shale. However, the mechanism of organic matter enrichment  
66 in the saline lacustrine basins remains unclear. Based on previous research findings and  
67 involved the development characteristics of organic-rich shale in Jiangnan Basin, this  
68 paper aims to elucidate the mechanism of organic matter enrichment in a saline  
69 lacustrine basin. The investigation encompasses hydrochemical conditions,  
70 sedimentation, biological activities, organic matter enrichment and consumption,  
71 aiming to provide a theoretical foundation for the development and prediction of high-  
72 quality shale in continental lacustrine basins, as well as shale oil exploration and  
73 development.

## 74 **2 SEDIMENTARY CHARACTERISTICS OF THE SALINE** 75 **LACUSTRINE BASIN**

76 Figure 2 illustrates the wide distribution of source rocks within China's saline  
77 lacustrine basins, spanning various geological periods. During the Permian period, the  
78 Junggar Basin and Santanghu Basin developed a semi-enclosed saltwater lake  
79 sedimentary environment under the compressive tectonic background (Du et al., 2020).  
80 Notably, two sets of high-quality source rocks were formed within the Fengcheng and  
81 Lucaogou Formations (Fan et al., 2021; He et al., 2021; Su et al., 2019). During the  
82 Cretaceous period, the Yin'e Basin and Erlian Basin experienced a brackish water to  
83 saltwater lake sedimentation in faulted depression settings, giving rise to high-quality  
84 source rocks within Bayingebi Formation. (Yu et al., 2021; Zhang et al., 2020). In the

85 Paleogene period, the development of China's saline lacustrine basin reached its peak,  
86 resulting in the formation of high-quality source rocks. The Bohai Bay Basin harbored  
87 such source rocks within the Shahejie Formation and Kongdian Formation, while the  
88 Subei Basin contained them within the Funing Formation. The Qaidam Basin exhibited  
89 high-quality source rocks within the Ganchaigou Formation and Dameigou Formation,  
90 whereas the Nanxiang Basin contained them within the Hetaoyuan Formation. Lastly,  
91 the Jiangnan Basin featured high-quality source rocks within the Qianjiang Formation  
92 and Xingouzui Formation (Li et al., 2021; Song et al., 2019; Wang et al., 2020; Zhang  
93 et al., 2019; Zhou et al., 2020).

94 In contrast to the relatively stable chemical composition found in the present-day  
95 marine environment, the composition of ions in the continental lacustrine basin water  
96 is complex and diverse. These ions originate from various sources, including  
97 atmospheric water, surface runoff water, transgressive residual water, and deep hot  
98 brine. Typically, the concentration of original salts in lake basins is relatively low, and  
99 the formation of saline lacustrine basin necessitates a combination of closed water  
100 bodies and strong concentration processes.

101 Under arid climate conditions, the evaporation of lake water surpasses the  
102 replenishment of rainfall or river water, resulting in the gradual shrinkage of the lake  
103 basin, salinization, and the deposition of corresponding salt minerals (Du et al., 2020;  
104 Wang et al., 2021; Yuan, 2019). Deep brine, which is rich in salt substances, contributes  
105 to the increased concentration of salts in lake basin water. Consequently, salt minerals  
106 are deposited, even without a high initial water concentration (Wu et al., 2017).

107           The composition of ions in saline lacustrine basin varies, leading to the deposition  
108 of different salt minerals during the process of evaporation and concentration. As the  
109 concentration and salinity in saline lacustrine basin increase, the initial precipitates are  
110 typically Ca-Mg carbonate minerals. In addition, based on the ratio of  $\text{Ca}^{2+}$  to  $\text{Mg}^{2+}$  in  
111 the brine, various minerals such as low magnesium calcite, high magnesium calcite,  
112 aragonite, and dolomite may form. This marks the primary stage of salinization in the  
113 lake (Figure 3; Warren, 2016). Representative strata illustrating this process include the  
114 Shahejie Formation in Dongying Sag of Bohai Bay Basin (Figure 4A) and 7<sup>th</sup> member  
115 of Dameigou Formation in Yuqia Sag of Qaidam Basin. These formations are  
116 characterized by the presence of mudstone and calcareous mudstone (Bai et al., 2021;  
117 Wang et al., 2019; Zhang et al., 2019). The subsequent deposition of minerals is  
118 determined by the ratio of  $\text{Ca}^{2+}$ ,  $\text{Mg}^{2+}$ , and  $\text{HCO}_3^-$  (Figure 3; Warren, 2016). When  
119  $(\text{Ca}^{2+}+\text{Mg}^{2+}) \gg \text{HCO}_3^-$ , the excess  $\text{Ca}^{2+}$  and  $\text{Mg}^{2+}$  ions, following the deposition of Ca-  
120 Mg carbonate minerals, combined with sulfate ions to precipitate abundant sulfate  
121 minerals, including gypsum and glauberite (Figure 4B1-B4). This stage is characterized  
122 by the process of sulfate brine, representing the process of seawater concentration  
123 sequence.

124           An example of such a stratum is the Xingouzui Formation in Jiangnan Basin  
125 (Figure 4A), which exhibits the development of three main lithological associations.  
126 The first association comprises argillaceous dolomite and dolomitic mudstone,  
127 reflecting the sedimentary characteristics during the early stage of salinization. The  
128 second association consists of interbedded argillaceous dolomite, dolomitic mudstone,  
129 and layered glauberite, indicating a further increase in water salinity. The third  
130 association features a pure glauberite section and locally visible salt rock, exemplifying

131 the sedimentary characteristics of late-stage salinization. When  $\text{HCO}_3^- \gg \text{Ca}^{2+} +$   
132  $\text{Mg}^{2+}$ , the brine exhibits a carbonate type. During the deposition stage of Ca-Mg  
133 carbonate minerals,  $\text{Ca}^{2+}$  and  $\text{Mg}^{2+}$  become depleted. At this time, the excessive  
134  $\text{HCO}_3^-$  combines with  $\text{Na}^+$  to form alkaline minerals, typically without the formation  
135 of gypsum and other sulfate minerals. An example of such a stratum is the Lower  
136 Permian Fengcheng Formation in the Mahu Sag of Junggar Basin. The sedimentary  
137 period of the Fengcheng Formation was characterized by frequent volcanic activities,  
138 which promoted the the high partial pressure of  $\text{CO}_2$  in the atmosphere. Consequently,  
139 a large amount of  $\text{CO}_2$  dissolved in the sedimentary water, resulting in the formation  
140 of  $\text{HCO}_3^-$ . The Fengcheng Formation showcases a complete alkaline lake sedimentary  
141 sequence (Figure 4A). In the first member of Fengcheng Formation, mudstone and  
142 dolomite were the primary minerals, with localized deposition of sodium carbonate  
143 minerals. As water salinity increased, the second member witnessed the emergence of  
144 numerous alkaline minerals, including reedmergnerite, shortite, eitelite, wegscheiderite  
145 and nahcolite (Figure 4C1-C4). Gradually, the content of dolomite and alkaline  
146 minerals decreased during the third member of Fengcheng Formation, indicating a  
147 weakening alkaline lake environment. (Cao et al., 2020).

## 148 **3 BIOLOGICAL ACTIVITY OF THE SALINE LACUSTRINE** 149 **BASIN**

### 150 **3.1 Biological species**

151 Previous studies initially suggested that that high salinity environments were



152 unfavorable for the survival of organisms. However, further research has revealed that  
153 biomass in these environments may not be reduced and can even be higher. The  
154 predominant organisms found in high salinity environments include microeukaryotes,  
155 halophilic bacteria and haloarchaea. For example, various algal groups, particularly  
156 diatoms, are consistently found in Qinghai Lake throughout the year (Yao et al., 2011),  
157 and halophilic bacteria and *Dunaliella* are commonly observed in large salt lakes in the  
158 United States (Baxter & Zalar, 2019). Significantly, extensive evidence of biological  
159 activities has been discovered in the source rock development strata of the saline  
160 lacustrine basins. For instance, in the organic-rich shale of the 7<sup>th</sup> member of the  
161 Dameigou Formation in Qaidam Basin, numerous biological fossils and algal bodies  
162 suspected resembling coccolithophores have been found, along with a substantial  
163 amount of biogenic apatite (Figure 5A-F). Zhang et al. (2019) identified organic-rich  
164 shales of Shahejie Formation in Dongpu Sag of Bohai Bay Basin by optical microscopy  
165 and scanning electron microscopy, and found many dinoflagellates, cyanobacteria,  
166 green algae and charophytes. Xia et al. (2022) confirmed the presence of *Dunaliella* in  
167 the shale of Fengcheng Formation in the Mahu Sag, Junggar Basin using organic  
168 geochemical indicators such as the C<sub>28</sub>/C<sub>29</sub> sterane ratio and β-carotene index.

### 169 **3.2 Biological survival mechanism**

170 Organisms in a salt lake require abundant nutrients for their survival. In high  
171 salinity environments, nitrogen and phosphorus compounds are crucial nutrients that  
172 promote the phytoplankton proliferation. A salinity increasing in evaporative

173 environments, nutrients become more concentrated. Therefore, even a slight increase  
174 in nutrient availability in saline environments can trigger a bloom of phytoplankton  
175 bloom (Jiang et al., 2004). Particularly in alkaline lake water with high pH levels, the  
176 presence of abundant CO<sub>2</sub>, molybdenum (Mo), and phosphorus (P) elements greatly  
177 facilitates biological reproduction (Li et al., 2021). In a saline environment, organisms  
178 face a significant challenge posed by osmotic pressure resulting from elevated salinity  
179 levels. Under normal circumstances, cells tend to lose water and ultimately succumb to  
180 the detrimental effects of such high osmotic pressure. However, organisms inhabiting  
181 lacustrine basins have evolved two distinct mechanisms to effectively maintain stable  
182 osmotic pressure and thrive in this challenging environment.

183         The first mechanism is referred to as the internal salt mechanism, which involves  
184 the accumulation of substantial quantities of potassium ions (K<sup>+</sup>) within cells until the  
185 intracellular reaches equilibrium with the concentration of ions (Na<sup>+</sup>) present in the  
186 surrounding environment. These accumulated K<sup>+</sup> ions facilitate the positioning of  
187 acidic amino acid residues on the surface of proteins and enzymes, leading to the  
188 formation of water layers that effectively prevent the collision and agglutination of  
189 macromolecules. This protective mechanism ensures that cells can carry out their  
190 normal physiological functions unhindered. It is particularly well-suited for halophilic  
191 microorganisms that require continuous survival in high salinity conditions. The second  
192 is mechanism is known as the compatible solute mechanism. Compatible organic  
193 solutes are small molecules, such as glycerol, that readily dissolve in water and do not  
194 negatively interfere with the enzymatic activity within cells. Some of these solutes are

195 synthesized within the cells themselves, while others are absorbed from the surrounding  
196 environment. Importantly, compatible organic solutes can be adjusted in response to the  
197 salinity of the external environment. This adaptability makes them particularly suitable  
198 for organisms residing in environments characterized by frequent fluctuations in  
199 salinity levels. Through the utilization of these mechanisms, including the internal salt  
200 mechanism and the employment of compatible solutes, organisms in saline  
201 environments can effectively mitigate the adverse effects of high osmotic pressure and  
202 thrive in extreme conditions (Han Shuaibo, 2021; Strahl & Greie, 2008).

## 203 **4 ORGANIC MATTER ENRICHMENT OF THE SALINE** 204 **LACUSTRINE BASIN**

### 205 **4.1. Biological bloom and primary productivity**

206 As salinity increases in saline lacustrine basins, there is a significant decrease in  
207 the number of species present. However, organisms that are adapted to specific salinity  
208 ranges can proliferate in these environments, benefiting from reduced competition for  
209 nutrients and living space, as well as the absence of predators. When the salinity of lake  
210 basin water changes and falls outside the optimal range for these organisms, a large  
211 number of these organisms will die (Figure 6). Barbe et al. (1990) conducted a study  
212 on seawater with different salinities in coastal areas, revealing that different salinity  
213 levels lead to the production of distinct groups of organisms.. For instance, when  
214 seawater salinity rises from 60‰ to 140‰, salt-tolerant organisms such as diatoms,  
215 green algae and cyanobacteria flourish. As the salinity further increases to around

216 300‰, the brine shrimp (*Artemia*), *Dunaliella*, halophilic archaea and eubacteria  
217 dominate (Figure 6A). It's important to note that the development of organisms in saline  
218 environments is influenced not only by salinity but also by factors such as light,  
219 temperature, nutrient availability. The aqueous conditions of lakes are highly sensitive  
220 to changes in structure, climatic, and source-related factors (Deng et al., 2020).  
221 Consequently, the salinity of lake basin water can undergo significant changes, ranging  
222 from freshwater to hypersaline conditions. These fluctuations, combined with other  
223 factors, can trigger sudden flourishing of certain species (biological blooms) followed  
224 by rapid die-offs (organic matter enrichment) (Figure 6B, 6C). Algae and bacteria  
225 involved in these processes are often rich in lipids, and their autolysis can directly  
226 contribute to the generation of hydrocarbons, thereby influencing the early stages of  
227 organic-rich shale formation (Guo, 1998). In the investigation of source rocks in saline  
228 lacustrine basins, has been observed that laminations are commonly developed,  
229 consisting of carbonate laminae, clay laminae and organic laminae (including algal  
230 laminae and biological fossil laminae) (Figure 7). Zheng et al. (1985) conducted  
231 research on Zabuye Salt Lake in Tibet and found that halophilic bacteria and algae are  
232 distributed extensively, forming organic matter enrichment layers of 1-2 cm thickness  
233 after their death. Zeng et al. (2017) proposed that fine organic laminae are generated by  
234 the extensive growth of benthic microbial communities during periods of nutrient  
235 abundance and high water salinity. Zhao et al. (2019) studied the laminated shale of the  
236 Shahejie Formation in Dongying Sag using astronomical cycle theory and concluded  
237 that these laminated shales represent annual laminae primarily influenced by seasonal

238 climate variations. Drawing from these investigations, it is hypothesized that the  
239 organic matter laminae observed in organic-rich shale within saline lacustrine basins  
240 may serve as a record of biological blooms that have adapted to specific water salinity  
241 conditions. These laminae provide valuable insights into the dynamics of past  
242 ecological processes within these environments.

#### 243 **4.2. Water stratification and organic matter preservation**

244 Previous research has indicated that when a lake reaches a certain depth, the water  
245 column undergoes stratification due to variations in density and gravity. The denser  
246 high salinity water occupies the bottom of the lake basin, while the less dense low  
247 salinity water resides at the surface, with the halocline separating the two layers. The  
248 surface water benefits from contact with the atmosphere, resulting in higher oxygen  
249 levels, and light penetration supports photosynthesis. Algae in the surface water exhibit  
250 the highest productivity and contribute the most to organic matter production, followed  
251 by bacteria near the halocline (Figure 7A). In the deep water of the lake basin, limited  
252 exchange occurs between the oxygenated surface water and the deep water due to the  
253 presence of the halocline. Consequently, the bottom water is characterized by a stagnant,  
254 anoxic, and strongly reducing environment (Figure 7A). The stratified water structure  
255 of the saline lacustrine basins provides favorable conditions for the preservation of  
256 organic matter (Jin et al., 2008), thus promoting the formation of high-quality source  
257 rocks. Based on available data, the preservation efficiency of marine organic matter in  
258 the modern shallow open oxygenated oceans is estimated to be approximately 0.1%

259 (Menzel & Ryther, 1970), In contrast, in the anoxic Black Sea, the preservation  
260 efficiency is around 4% (Warren, 2016). Notably, in high-salinity lakes with density-  
261 stratified water bodies, the preservation efficiency of organic matter can reach a  
262 remarkable 85% (Hite & Anders, 1991). Comparing two modern lake basins, namely  
263 the mesotrophic Qinghai Lake and the eutrophic Turkana Lake, both characterized by  
264 brackish water environments, reveals interesting differences. Despite Turkana Lake  
265 having relatively high nutrient levels and surface productivity, the average organic  
266 matter content in the lake's bottom is only about 0.6%. In contrast, Qinghai Lake, with  
267 its stratified water conditions, exhibits an average organic matter content of 2.29% in  
268 the bottom sediments. These findings highlight the significance of water stratification  
269 and strong reduction preservation conditions in the bottom sediments for the  
270 enrichment of organic matter in high-salinity lakes.

## 271 5 ORGANIC MATTER CONSUMPTION OF THE SALINE 272 LACUSTRINE BASIN

273 According to the research conducted by Jiang et al. (2004), it has been observed  
274 that during the development, evolution, and sedimentation of the saline lacustrine basin,  
275 the early stages characterized by Ca-Mg carbonate sedimentation exhibit organic matter  
276 enrichment that is approximately three orders of magnitude higher compared to the later  
277 stages characterized by sulfate and halide sedimentation. In China, source rocks formed  
278 under a typical sulfate saline lake setting also exhibit low organic matter content,  
279 indicating that the late evolution of the saline lacustrine basins may not be favorable for  
280 organic matter enrichment. This reason phenomenon could be attributed to factors such  
281 as sulfate reduction during early diagenetic stage and the deposition rate of salt rock.5.1.  
282 Bacterial sulfate reduction (BSR)

283 In anoxic environments, sulfate-reducing bacteria (SRB) utilize sulfate ions ( $\text{SO}_4^{2-}$ )  
284 as electron donors to metabolize organic matter at temperatures below 60-80°C. During  
285 this process, sulfate is reduced to H<sub>2</sub>S gas or further forms pyrite (Strauss, 1999).  
286 Reeburgh (1980) suggested that microbial sulfate oxidation of organic matter is more  
287 pronounced compared to other oxidants such as oxygen, nitrate, and metal oxides. Kelts  
288 (2015) indicated that the efficiency of sulfate oxidation of organic matter in lakes  
289 primarily depends on sulfate concentration. For instance, in Vechten Lake, which has a  
290 sulfate concentration of approximately 15g/m<sup>3</sup>, around 25% of the sedimentary organic  
291 matter is degraded annually. Bacterial sulfate reduction (BSR) leads to the enrichment

292 of residual sulfate relatively higher  $\delta^{34}\text{S}$  values (Wang et al., 2014). Canfield et al.  
293 (1996) reported a sulfur isotope fractionation range of 4‰ ~ 46‰, resulting from BSR,  
294 with an average of 21‰. However, in the absence of sulfate-reducing bacteria, the  $\delta^{34}\text{S}$   
295 value of sulfate in lake basin water is significantly lower, approximately 20‰ (Zhang  
296 et al., 2010). Xiao et al. (2020) found that the difference of  $\delta^{34}\text{S}$  value between  $\text{H}_2\text{S}$   
297 produced after BSR and the original  $\text{SO}_4^{2-}$  ranged from -15‰ and -30‰. Sulfur isotope  
298 analysis of organic-rich shale in Xingouzui Formation, Jiangnan Basin indicated that  
299 the  $\delta^{34}\text{S}$  values of the original  $\text{SO}_4^{2-}$  and the generated  $\text{H}_2\text{S}$  were 26.4 ~ 40.1‰ and  
300 12.0 ~ 32.0‰ respectively. The difference of  $\delta^{34}\text{S}$  between generated  $\text{H}_2\text{S}$  and  
301 original  $\text{SO}_4^{2-}$  ranges from -27.0 to -19.5‰ (Xiao et al., 2020). These findings highlight  
302 the significant impact of BSR on the consumption of sedimentary organic matter, which  
303 aligns with the relatively high sulfate content and low abundance of organic matter  
304 observed in the Xingouzui Formation shale in the Jiangnan Basin (Li et al., 2021,  
305 2022).

### 5.2. Thermochemical sulfate reduction (TSR)

306 During the later stage of diagenesis, a process called thermochemical sulfate  
307 reduction (TSR) occurs when the burial temperature a specific range and there is  
308 sufficient contact between sulfate and organic matter. Previous studies have indicated  
309 that TSR typically occurs at temperatures between 100~200°C, which coincides with  
310 the formation temperature of light oil and condensate (Bildstein et al., 2001). In the  
311 lower member of the Xingouzui Formation in the Jiangnan Basin, shale sections can be  
312 distinguished into three high total organic carbon (TOC) sections and two low TOC  
313 sections (Figure 8A). The high TOC sections consist mainly of dolomitic mudstone,



314 while the low TOC sections comprise numerous thinly thin layered glauberite ( $\text{Na}_2\text{Ca}$   
315  $(\text{SO}_4)_2$ ) and dolomitic mudstone interbeds (Figure 8A, 8B). The organic-rich shale in  
316 the Xinguozui Formation in Jiangnan Basin has reached mature stage, as indicated by  
317 a vitrinite reflectance ( $R_o$ ) is 0.7-1.2%, corresponding to the stage of significant  
318 hydrocarbon generation. In the shales of Xingouzui Formation, glauberite frequently  
319 occurs as interbeds with organic-rich shales, exhibiting high sulfate content and  
320 directcontact with organic matter. These conditions are conducive to TSR, which  
321 contributes to the consumption of organic matter and aligns with the relatively low  
322 abundance of organic matter observed in the Xingouzui Formation shale (Li et al., 2021,  
323 2022). Additionally, significant pyrite mineralization is present in the shales of  
324 Xingouzui Formation, with pyrite particle sizes averaging around 5 microns, some of  
325 which are associated with organic matter (Figure 8C). Wang et al. (2015) proposed that  
326 pyrite is a product of TSR. In summary, thermochemical sulfate reduction (TSR) during  
327 late diagenesis period of saline lacustrine shale represents another important  
328 mechanism for organic matter consumption and abundance reduction.

### 329 **5.3. Deposition rate**

330 The deposition rate plays a significant role in the enrichment of organic matter  
331 (Figure 9). When the deposition rate is low, organic matter will remains exposed to an  
332 oxidation environment for an extended period, increasing the likelihood of complete  
333 consumption by oxidation, which is unfavorable for organic matter preservation  
334 (Henrichs & Reeburgh, 1987). As the deposition rate increases, organic matter

335 experiences a shorter time in oxygenated water, enhancing its preservation (Müller &  
336 Suess, 1979). However, when the deposition rate is excessively fast, inorganic minerals  
337 are rapidly deposited in sediments, resulting in limited organic matter being diluted by  
338 a large number of inorganic minerals. This situation hampers the organic matter  
339 preservation (Ibach, 1980). Tyson (2001) suggested that the critical threshold for  
340 excessive deposition rate of marine organic matter enrichment is 5 cm/ka. Ding et al.  
341 (2017), in their study of the Tenger Formation in the Erlian Basin, also identified 5  
342 cm/ka as the critical threshold for excessive deposition rate in organic matter  
343 enrichment. According to Jiang et al. (2004), the deposition rates of the Qianjiang  
344 Formation in the Qianjiang Sag of the Jiangnan Basin and the Shahejie Formation in  
345 the Dongpu Sag of Bohai Bay Basin, both with a sulphate-type salt lake sedimentary  
346 background, are 32 cm/ka and 29 cm/ka, respectively (Table 1), significantly higher  
347 than the critical threshold deposition rate (Figure 9A). Hofman et al. (1993) pointed out  
348 that the deposition rate of anhydrite was 156.2 cm/ka, while of salt rock was 3030 cm/ka,  
349 thereby increasing the dilution effect of inorganic minerals on organic matter.  
350 Furthermore, in the later stages of the evolution of the saline lacustrine basin evolution,  
351 the water density increases, making it difficult for organic matter to settle rapidly and  
352 rendering it more susceptible to oxidation. Hence, higher deposition rate in the late  
353 stage of saline lacustrine evolution lead to a dilution effect on organic matter, which is  
354 unfavorable for its enrichment. Thus understanding aligns with the relatively high  
355 content of salt minerals and low abundance of organic matter observed in the shales of  
356 the Xingouzui Formation in the Jiangnan Basin (Li et al., 2021, 2022).

## 357 **6 HYDROCARBON GENERATION OF ORGANIC MATTER IN** 358 **THE SALINE LACUSTRINE BASIN**

359 The salt minerals in saline lacustrine basins exists in two primary forms: giant  
360 thick gypsum salt beds formed through long-term deposition in saline lake  
361 environments and thin beds of salt rock interbedded with mud shale s. Both have  
362 important effects on the hydrocarbon generation and evolution of source rocks (Carroll  
363 & Bohacs, 2001; Qi et al., 2021). The giant thick gypsum salt beds exhibit high thermal  
364 conductivity, typically 2~3 times that of sand and mudstone (Qiu et al., 2004). This  
365 characteristic facilitates the transfer of deep heat to the shallow regions. In the Shahejie  
366 Formation of the Dongpu Sag in the Bohai Bay Basin, the strata adjacent to the upper  
367 part of the gypsum salt beds exhibit significantly higher temperatures compared to areas  
368 without gypsum salt layers at the same depth. Conversely, the strata below the gypsum  
369 salt layer show notably lower temperatures than areas without gypsum salt beds at the  
370 same depth. This observation indicates the efficient heat conduction of gypsum salt  
371 beds. (Li, 2018), which promotes the hydrocarbon generation in overlying source rock.  
372 Chen et al. (2018) conducted a comparative study on the influence of different thickness  
373 of gypsum salt beds on the hydrocarbon generation threshold of source rocks. They  
374 concluded that a minimum thickness of 50 meters of gypsum salt beds is necessary to  
375 impact the hydrocarbon generation of source rocks. In the case of source rocks  
376 interbedded with thin salt rocks, it is commonly believed that salt minerals can affect  
377 and modify the charge distribution on the surface of kerogen molecules through solvent  
378 effect and electron induction effect, thus reducing the C-C bond energy (Li et al., 2002),

379 This alteration can impact the hydrocarbon generation of the source rock. Through the  
380 hydrocarbon generation simulation experiments and computer molecular simulations,  
381 Ban (2018) obtained the variation of dissociation energy with salinity and generated a  
382 chart illustrating the hydrocarbon production rate of source rocks in a saline lacustrine  
383 basin (Figure 10). The chart shows that higher-quality organic matter and higher salinity  
384 contribute to higher hydrocarbon content. Changes in salinity have a more pronounced  
385 effect on the hydrocarbon generation of type III kerogen than compared to type I  
386 kerogen (Figure 10).

387 In sulfate-type lake basin, the activation energy of the S-C/S-S bonds, which are  
388 abundant in high sulfur kerogen, is lower than that of C-C and C-O bonds, making them  
389 easier to break at low temperatures. This characteristic promotes the early generation  
390 of hydrocarbons. Ma et al. (2013) conducted hydrocarbon generation and expulsion  
391 simulation experiments on saline and non-saline shale samples from the Dongpu Sag,  
392 Bohai Bay Basin. The results showed that the oil expulsion rate from saline samples  
393 was much higher than that from non-saline samples. This is primarily due to the  
394 existence of salt minerals, which reduces the internal adsorption capacity of the source  
395 rock and facilitates expulsion of hydrocarbons (Figure 11). Therefore, the gypsum salt  
396 rocks formed in the saline lacustrine basins not only promote the hydrocarbon  
397 generation of organic matter but also facilitate the expulsion of hydrocarbon expulsion  
398 of source rock.

## 399 7 CONCLUSIONS

400 The source rocks in saline lacustrine basins in China are diverse and span a wide  
401 geological time range, making them important for shale oil exploration. Saline  
402 lacustrine basins undergo different stages of development and sedimentation, resulting  
403 in the formation of various salt minerals. These include Ca-Mg carbonates in the early  
404 salinization stage, sulfate minerals like gypsum and calcium glauberite in the late  
405 salinization stage, and alkaline minerals such as reedmergnerite and nahcolite when  
406  $\text{HCO}_3^-$  ions dominates over  $\text{Ca}^{2+}$  and  $\text{Mg}^{2+}$  ions.

407 Saline lacustrine basins host a wide variety of biological organisms and exhibit  
408 extensive biological activities. Algae, microorganisms, halophilic bacteria, and  
409 halophilic archaea are abundant in these basins, with their proliferation supported by  
410 the saline environment and mechanisms like internal salt accumulation. This biological  
411 activity contributes to the enrichment of sedimentary organic matter in the basins. The  
412 enrichment process involves biological bloom and primary productivity, as well as  
413 water stratification and organic matter preservation. Fluctuations in salinity due to  
414 climate and environmental changes can lead to episodes of rapid organism flourishing  
415 and subsequent death, creating favorable conditions for organic matter enrichment. The  
416 water stratification in saline lacustrine basins promotes the preservation of sedimentary  
417 organic matter through bottom water anoxia.

418 Furthermore, salt minerals play a significant role in hydrocarbon generation and  
419 expulsion within saline lacustrine basins. Thick gypsum salt beds have high thermal  
420 conductivity, facilitating the thermal evolution and hydrocarbon generation of

421 overlying source rocks. In source rocks interbedded with thin salt rocks, salt minerals  
422 impact the charge distribution on kerogen molecules, reducing C-C bond energy and  
423 promoting hydrocarbon generation. Salt minerals also reduce the internal adsorption  
424 capacity of source rocks, facilitating the expulsion of hydrocarbons. Overall, saline  
425 lacustrine basins provide favorable conditions for the generation and expulsion of  
426 hydrocarbons from organic-rich shales.

## 427 **ACKNOWLEDGMENTS**

428 This research was supported by the Shandong Provincial Key Research and  
429 Development Program (2020ZLYS08), the National Natural Science Foundation of  
430 China (42122017, 41821002), the independent innovation research program of China  
431 University of Petroleum (East China) (21CX06001A), and the fundamental research  
432 fund from China University of Geosciences, Wuhan.

## 433 **REFERENCES**

- 434 Bai, N., Xu, S., Wang, Y., Guo, T., & Shi, W. (2021). Facies Characteristics and Sedimentary  
435 Evolution Model of the 7<sup>th</sup> Member of Dameigou Formation in Yuqia Area, North Qaidam  
436 Basin. *Northwestern Geology*, 54(02),74-85. (in Chinese with English abstract).
- 437 Ban, D. (2018). *Hydrocarbon generation pattern of Neogene salinized lacustrine source rocks in*  
438 *Yiliping Area, Qaidam Basin*. China University of Petroleum Beijing, 2018. (in Chinese with  
439 English abstract).
- 440 Barbe, A., Grimalt J., Pueyo J., et al. (1990). Characterization of model evaporitic environments  
441 through the study of lipid components. *Organic Geochemistry*, 16(4-6), 815-828.
- 442 Baxter, B. K., & Zalar, P. (2019). Chapter 4. The extremophiles of Great Salt Lake: Complex  
443 microbiology in a dynamic hypersaline ecosystem. In: *Astrobiology Exploring Life on Earth*  
444 *and Beyond*, 57-99.

445 Bildstein, O., Worden, R.H., & Brosse, E. (2001). Assessment of anhydrite dissolution as the rate-  
446 limiting step during thermochemical sulfate reduction. *Chemical Geology*, 176(1-4), 173-189.

447 Canfield, D.E., et al. (1996), Late Proterozoic rise in atmospheric oxygen concentration inferred  
448 from phylogenetic and ??? *Nature*, 382, 127-132.

449 Cao, J., Lei, D., Li, Y., Tang, Y., Chang, Q., & Wang, T. (2015). Ancient high-quality alkaline  
450 lacustrine source rocks discovered in the Lower Permian Fengcheng Formation, Junggar Basin.  
451 *Acta Petrolei Sinica*, 36(7), 781-790. (in Chinese with English abstract).

452 Cao, J., Xia, L., Wang, T., et al. (2020). An alkaline lake in the Late Paleozoic Ice Age (LPIA): A  
453 review and new insights into paleoenvironment and hydrocarbon potential. *Earth-Science*  
454 *Reviews*, 202(1), 103091

455 Carroll, A.R., & Bohacs, K.M. (2001). Lake-type controls on petroleum source rock potential in  
456 nonmarine basins. *AAPG Bulletin*, 85(6), 1033–1053.

457 Deng Yuan, Chen Shiyue, Pu Xiugang, Yan Jihua, Chen Jia. Formation mechanism and  
458 environmental evolution of fine-grained sedimentary rocks from the second member of  
459 Kongdian Formation in Cangdong Sag, Bohai Bay Basin [J]. *Oil & Gas Geology*, 2020, 41(04):  
460 811-823+890. (in Chinese with English abstract).

461 Ding Xiujian, Liu Guangdi, Zha Ming, et al. Relationship between total organic carbon content and  
462 sedimentation rate in ancient lacustrine sediments, a case study of Erlian basin, northern  
463 China[J]. *Natural Gas Geoscience*, 2015, 26(6):1076-1085.

464 Ding Xiujian, Liu Guangdi, Zhao Longmei, Gao Dengkuan, Zhang Kai, Kuang Daqing. Organic  
465 Matter Enrichment and Hydrocarbon Source Rock Forming Mechanism in Small-Scale Faulted  
466 Lacustrine Basins: A Case from the First Member of Lower Cretaceous Tenger Formation in  
467 Erlian Basin [J]. *Xinjiang Petroleum Geology*, 2017, 38(06): 650-657. (in Chinese with English  
468 abstract).

469 Du Jiangmin, Long Pengyu, Yang Peng, Ding Qiang, Hu Xiugen, Li Wei, Bo Yang, Sheng Jun.  
470 Characteristics of Carbonate Reservoir and Its Forming Conditions in Continental Lake Basin  
471 of China [J]. *Advances in Earth Science*, 2020, 35(01): 52-69. (in Chinese with English  
472 abstract).

473 Fan Tanguang, Xu Xiongfei, Fan Liang, Fan Yaqin, Liu Wenhui, Liu Juntian, Wang Meiyang, Jia  
474 Guoqiang. Geological characteristics and exploration prospect of shale oil in Permian

475 Lucaogou Formation, Santanghu Basin [J]. *China Petroleum Exploration*, 2021, 26(04): 125-  
476 136. (in Chinese with English abstract).

477 Guo Shaohui. *Geo-macromolecular Structure of Organic Matter in Immature Source Rocks and the*  
478 *Mechanism of Immature Petroleum Formation* [D]. the University of Petroleum China, 1998.  
479 (in Chinese with English abstract).

480 He Wenjun, Qian Yongxin, Zhao Yi, Li Na, Zhao Xinmei, Liu Guoliang, Miao Gang. Exploration  
481 Implications of Total Petroleum System in Fengcheng Formation, Mahu Sag, Junggar Basin  
482 [J]. *Xinjiang Petroleum Geology*, 2021,42(06): 641-655. (in Chinese with English abstract).

483 Henrichs Susan M and Reeburgh William S. Anaerobic mineralization of marine sediment organic  
484 matter: Rates and the role of anaerobic processes in the oceanic carbon economy[J].  
485 *Geomicrobiology Journal*, 1987, 5(3-4):191-237.

486 Hite R J and Anders D E. Petroleum and evaporites[J]. *Evaporites Petroleum & Mineral Resources*,  
487 1991, 50:477-533.

488 Hofmann P, Leythaeuser D, Carpentier B. Palaeoclimate controlled accumulation of organic matter  
489 in Oligocene evaporite sediments of the Mulhouse basin[J]. *Organic Geochemistry*, 1988,  
490 20(8):1125-1138.

491 Ibach LE Johnson. Relationship between sedimentation rate and total organic carbon content in  
492 ancient marine sediments[J]. *Am.assoc.pet.geol*, 1980, 66(2):170-188.

493 Jiang Jigang, Peng Pingan, Sheng Guoying. Formation, evolution, migration and accumulation of  
494 oil and gas in salt lakes [M]. Guangdong Science and Technology Press, 2004.

495 Jiang Jigang, Sheng Guoying, Fu Jiamo. Discovery of Immature High Sulfur Grude oil and its  
496 Significance in Gypsum-salt Bearing Sedimentary Basin [J]. *Petroleum Geology &*  
497 *Experiment*, 1988(04): 36-42. (in Chinese with English abstract).

498 Jin Qiang and Huang Xinghan. Studies on the Origin of the Early Tertiary Salt Lake Dongpu  
499 Depression – a Postulated Deep Water Model [J]. *Journal of East China Petroleum Institute*  
500 (Edition of Natural Science), 1985(01): 1-13. (in Chinese with English abstract).

501 Jin Qiang and Zhu Guangyou. Progress in Research of Deposition of Oil Source Rocks in Saline  
502 Lakes and Their Hydrocarbon Generation [J]. *Geological Journal of China Universities*,  
503 20016(04): 483-492. (in Chinese with English abstract).

504 Jin Qiang, Zhu Guangyou, Wang Juan. Deposition and distribution of high-potential source rocks in



505 saline lacustrine environments [J]. *Journal of China University of Petroleum (Edition of*  
506 *Natural Science)*, 2008(04): 19-23. (in Chinese with English abstract).

507 Kelts, K. *Environments of deposition of lacustrine petroleum source rocks: an introduction*[J].  
508 *Lacustrine Petroleum Source Rocks*, Geological Society Special Publication, 1988, 40:3-26.

509 Li Bei. *Origin of the salt rock of Shahejie Formation and its relationship with source Rock in*  
510 *Dongpu Depression* [D]. Northwest University, 2018. (in Chinese with English abstract).

511 Li Qiqi, Shang Xu, Liang Zhang, Fengling Chen, Shiqiang Wu, Nan Bai. *Shale oil enrichment*  
512 *mechanism of the Paleogene Xingouzui Formation, Jiangnan Basin, China*. *Energies*, 2022, 15:  
513 4038.

514 Li Qiqi, Xu Shang, Hao Fang, et al. *Geochemical characteristics and organic matter accumulation*  
515 *of argillaceous dolomite in a saline lacustrine basin: A case study from the paleogene xingouzui*  
516 *formation, Jiangnan Basin, China*[J]. *Marine and Petroleum Geology*, 2021, 128: 105041.

517 Li Shuyuan, Lin Shijing, Guo Shaohui, Liu Luofu. *Effects of inorganic salts on the hydrocarbon*  
518 *generation from kerogens* [J]. *GEOCHIMICA*, 2002, 31(1): 15-20. (in Chinese with English  
519 abstract).

520 Ma Zhongliang, Zheng Lunju, Li Zhiming, Qin Jianzhong. *The Effect of Salts on Hydrocarbon*  
521 *Generation and Expulsion of Argillaceous Source Rock* [J]. *Journal of Southwest Petroleum*  
522 *University (Science & Technology Edition)*, 2013, 35(01): 43-51. (in Chinese with English  
523 abstract).

524 Menzel D. W and Ryther J H. *Distribution and recycling of organic matter in the oceans*[J].  
525 *University of Alaska, Institute of Marine Science, Occasional Publication*, 1970, 1:31–53.

526 Müller P.J and Suess E. *Productivity, sedimentation rate, and sedimentary organic matter in the*  
527 *oceans—I. Organic carbon preservation*[J]. *Deep Sea Research Part A. Oceanographic*  
528 *Research Papers*, 1979, 26(12):1347-1362.

529 Qi Wen, Wu Jia, Xia Yanqing, et al. *Influence of ionic composition on minerals and source rocks:*  
530 *An investigation between carbonate-type and sulfate-type lacustrine sediments based on*  
531 *hydrochemical classification*[J]. *Marine and Petroleum Geology*, 2021, 130:105099.

532 Qiu Nansheng. *Theory and application of geothermal regime in sedimentary basin* [M]. *Petroleum*  
533 *Industry Press*, 2004.

534 Reeburgh William S. *Anaerobic methane oxidation: Rate depth distributions in Skan Bay*

535 sediments[J]. *Earth & Planetary Science Letters*, 1980, 47(3):345-352.

536 Song Yu, Li Shuifu, Hu Shouzhi. Warm-humid paleoclimate control of salinized lacustrine organic-  
537 rich shale deposition in the Oligocene Hetaoyuan Formation of the Biyang Depression, East  
538 China[J]. *International Journal of Coal Geology*, 2019, 202:69-84.

539 Strahl H, Greie J C. The extremely halophilic archaeon *Halobacterium salinarum* R1 responds to  
540 potassium limitation by expression of the K<sup>+</sup>-transporting KdpFABC P-type ATPase and by a  
541 decrease in intracellular K<sup>+</sup>[J]. *Extremophiles*, 2008, 12(6):741-752.

542 Strauss Harald. Geological evolution from isotope proxy signals-sulfur[J]. 1999, 161(1-3):0-101.

543 Su Yang, Zha Ming, Ding Xiujian, et al. Petrographic, palynologic and geochemical characteristics  
544 of source rocks of the Permian Lucaogou formation in Jimsar Sag, Junggar Basin, NW China:  
545 Origin of organic matter input and depositional environments[J]. *Journal of Petroleum Science  
546 and Engineering*, 2019, 183:106364.

547 Tyson R V. Sedimentation rate, dilution, preservation and total organic carbon: some results of a  
548 modelling study[J]. *Organic Geochemistry*, 2001, 32(2):333-339.

549 Wang Jiangong, Zhang Daowei, Yang Shaoyong, et al. Sedimentary characteristics and genesis of  
550 the salt lake with the upper member of the Lower Ganchaigou Formation from Yingxi sag,  
551 Qaidam basin[J]. *Marine and Petroleum Geology*, 2020, 111: 135-155.

552 Wang JunXian, Sun PingChang, Liu ZhaoJun, et al. Depositional environmental controls on the  
553 genesis and characteristics of oil shale: Case study of the Middle Jurassic Shimengou  
554 Formation, northern Qaidam Basin, north-west China[J]. *Geological Journal*, 2019, 55: 4585-  
555 4603

556 Wang Licheng, Liu Chenglin, Fei Mingming, Shen Lijian, Zhang Hua. Sulfur isotopic composition  
557 of sulfate and its geological significance of Yunlong formation in the Lanping Basin, Yunnan  
558 Province [J]. *China Mining Magazine*, 2014, 23(12): 57-65. (in Chinese with English abstract).

559 Wang Mengshi, Zhang Zhijie, Zhou Chuanmin, Yuan Xuanjun, Lin Minjie, Liu Yinhe, Cheng Dawei.  
560 Lithological characteristics and origin of alkaline lacustrine of the Lower Permian Fengcheng  
561 Formation in Mahu Sag, Junggar Basin [J]. *Journal of Palaeogeography (Chinese Edition)*,  
562 2018, 20(01): 147-162. (in Chinese with English abstract).

563 Wang Xiaojie, Zhang Shiqi, Wei Mengji, Mu Xiaoshui, Xu Tianwu. Characteristics and formation  
564 mode of Es<sub>3</sub> Member pyrite in Wendong Area of Dongpu Depression [J]. *Fault-Block Oil &*

565 Gas Field, 2015, 22(02): 178-183. (in Chinese with English abstract).

566 Wang Xiaojun, Song Yong, Guo Xuguang, Chang Qiusheng, Kong Yuhua, Zheng Menglin, Qin  
567 Zhijun, Yang Xiaofa. Classification of Fine-grained Sedimentary Rocks in Saline Lacustrine  
568 Basins and Its Petroleum Geological Significance [J/OL]. *Acta Sedimentologica Sinica*. (in  
569 Chinese with English abstract). DOI: 10.14027/j.issn.1000-0550.2021.080.

570 Wang Yuxuan, Xu Shang, Hao Fang, et al. Arid climate disturbance and the development of salinized  
571 lacustrine oil shale in the Middle Jurassic Dameigou Formation, Qaidam Basin, northwestern  
572 China [J]. *Palaeogeography, Palaeoclimatology, Palaeoecology*, 2021, 577:110533.

573 Warren J K. *Evaporites: A Geological Compendium*[M]. Springer, 2016.

574 Wu Xiaoli, Liu Hanlin, Li Rongxi, Li Delu, Zhao Bangsheng, Cheng Jinghua, Wei Jinglin, Zhu  
575 Qianping. Progress in Researches of Developmental Rule and the Hydrocarbon Generation and  
576 Expulsion Characteristics of Hydrocarbon Source Rocks in Terrestrial Evaporite Basins of  
577 China [J]. *Bulletin of Geological Science and Technology*, 2017, 36(04): 183-192. (in Chinese  
578 with English abstract).

579 Xia Liuwen, Cao Jian, Bian Lizeng, Hu Wenxuan, Wang Tingting, Zhi Dongming, Tang Yong, Li  
580 Erting. Co-evolution of paleo-environment and bio-precursors in a Permian alkaline lake,  
581 Mahu mega-oil province, Junggar Basin: Implications for oil sources. *Scientia Sinica (Terrae)*,  
582 2022, 52(04): 732-746. (in Chinese with English abstract).

583 Xiao Qi lin, Cai Suyang, Liu Jinzhong. Microbial and thermogenic hydrogen sulfide in the  
584 Qianjiang Depression of Jiangnan Basin: Insights from sulfur isotope and volatile organic  
585 sulfur compounds measurements. *Applied Geochemistry*, 2020:104865.

586 Yao Weizhi, Shi Jianquan, Qi Hongfang, Yang Jianxin, Jia Li, Pu Jiong. Study on the phytoplankton  
587 in Qinghai Lake during summer of 2006-2010. *Freshwater Fisheries*, 2011, 41(03): 22-28. (in  
588 Chinese with English abstract).

589 Yu Jiaqi, Liu Rong, Zhang Kun, Yan Xu. Organic geochemical characteristics and metallogenic  
590 conditions of oil shale of Lower Cretaceous Bayingebi Formation in Yin'e Basin. *World  
591 Geology*, 2021, 40(02): 330-342. (in Chinese with English abstract).

592 Yu Kuanhong, Cao Yingchang, Qiu Weilong, Sun Peipei, Yang Yongqiang, Qu Changsheng, Li  
593 Yuwen, Wan Min, Su Yunguo. Brine evolution of ancient lake and mechanism of carbonate  
594 minerals during the sedimentation of Early Permian Fengcheng Formation in Mahu Depression,

595 Junggar Basin, China. *Natural Gas Geoscience*, 2016, 27(07): 1248-1263. (in Chinese with  
596 English abstract).

597 Yuan Xiaoyu. *Sedimentation and Diagenesis of saline lacustrine from Qaidam Basine, Yinxi Area,*  
598 *Paleogene, Upper Xiaganchaigou Formation.* Lanzhou University, 2019. (in Chinese with  
599 English abstract).

600 Zeng Xiang, Cai Jingong, Dong Zhe, Wang Xuejun, Hao Yunqing. Sedimentary characteristics and  
601 hydrocarbon generation potential of mudstone and shale: a case study of Middle Submember  
602 of Member 3 and Upper Submember of Member 4 in Shahejie Formation in Dongying sag.  
603 *Acta Petrolei Sinica*, 2017, 38(01):31-43. (in Chinese with English abstract).

604 Zhang Hong, Huang Haiping, Li Zheng, et al. Oil physical status in lacustrine shale reservoirs – A  
605 case study on Eocene Shahejie Formation shales, Dongying Depression, East China[J]. *Fuel*,  
606 2019, 257: 116027.

607 Zhang Kun, Liu Rong, Liu Zhaojun, et al. Influence of palaeoclimate and hydrothermal activity on  
608 organic matter accumulation in lacustrine black shales from the Lower Cretaceous Bayingebi  
609 Formation of the Yin'e Basin, China. *Palaeogeography, Palaeoclimatology, Palaeoecology*,  
610 2020, 560: 110007.

611 Zhang Zhenguó, Gao Jilei, Zhang Xiangwen. Geochemistry of sulfur isotope of Paleo-Evaporites  
612 in Tarim Basin. *Gansu Geology*, 2010, 19(01): 32-37. (in Chinese with English abstract).

613 Zhao Ke, Du Xuebin, Lu Yongchao, et al. Are light-dark coupled laminae in lacustrine shale  
614 seasonally controlled? A case study using astronomical tuning from 42.2 to 45.4Ma in the  
615 Dongying Depression, Bohai Bay Basin, eastern China. *Palaeogeography, Palaeoclimatology,*  
616 *Palaeoecology*, 2019, 528:35-49.

617 Zheng Mianping, Liu Wengao and Xiang Jun. The Discovery of Halophilic Algae and Halobacteria  
618 at Zabuye Salt Lake Tibet and Preliminary Study on the Geology. *Acta Geologica Sinica*,  
619 1985(02): 162-171-188. (in Chinese with English abstract).

620 Zhou Xuewen, Jiang Zaixing, JamesA. MacEachern. Criteria for differentiating microbial caddisfly  
621 bioherms from those of marine polychaetes in a lacustrine setting: Paleocene second member,  
622 Funing Formation, Subei Basin, East China. *Palaeogeography, Palaeoclimatology,*  
623 *Palaeoecology*, 2020, 560: 109974.

624 **Figure captions**

625 FIGURE 1 Worldwide distribution of evaporite-related source rocks named with  
626 respect to hosting basins (from Warren, 2016)

627 FIGURE 2 Spatial and temporal distribution of source rocks in continental lacustrine  
628 basins of China. Abbreviations: P, Permian; T, Triassic; J, Jurassic; K, Cretaceous;  
629 E, Eocene, N, Neogene

630 FIGURE 3 Hydrologic classification and brine evolution pathways of concentrating  
631 non-marine waters and a listing of major evaporite minerals associated with the  
632 different brine types (from Warren, 2016)

633 FIGURE 4 (A) Lithologic histogram of different types of saline lacustrine basins; (B1-  
634 B4) sulphate core and its microscopic characteristics; (C1-C4) Na carbonate cores  
635 and microscopic features (Figure C1-C4 from Wang et al., 2018; Cao et al., 2015)

636 FIGURE 5 Characteristics of organic matter in shale of saline lacustrine basin. (A)  
637 Coccolithophores; (B) Coccolithophores; (C) Coccolithophores (cross-extinction);  
638 (D) algophytes; (E) algophytes; (F) apatite

639 FIGURE 6 (A) Biological development of seawater with different salinities; (B)  
640 Mechanisms of biogenesis with salinity; (C) Relationship between species and  
641 biomass as salinity changes (Figure A modified from Barbe et al., 1990; Figure B  
642 and C modified from Warren, 2016)

643 FIGURE 7 (A) Organic matter enrichment mechanism in stratified water; (B) Source  
644 rock laminar structure of saline lacustrine basin

645 FIGURE 8 (A) Comprehensive histogram of the seventh Member of Dameigou

646 Formation; (B) Core photos of the seventh member of Dameigou Formation; (C)

647 Pyrite

648 FIGURE 9 Relationship between deposition rate and organic carbon content (modified

649 from Ding et al., 2015)

650 FIGURE 10 Effects of salts on hydrocarbon generation of different kerogens (modified

651 from Ban, 2018)

652 FIGURE 11 Simulation of hydrocarbon generation and expulsion from saline and non-

653 saline shale samples (modified from Ma et al., 2013)

654 **Table captions**

655 Table 1 Sedimentary rate of tertiary partially saline lacustrine basin (data from Jiang et

656 al., 2004)



Figure 1 Worldwide distribution of evaporite-related source rocks named with respect to hosting basins (from Warren, 2016)

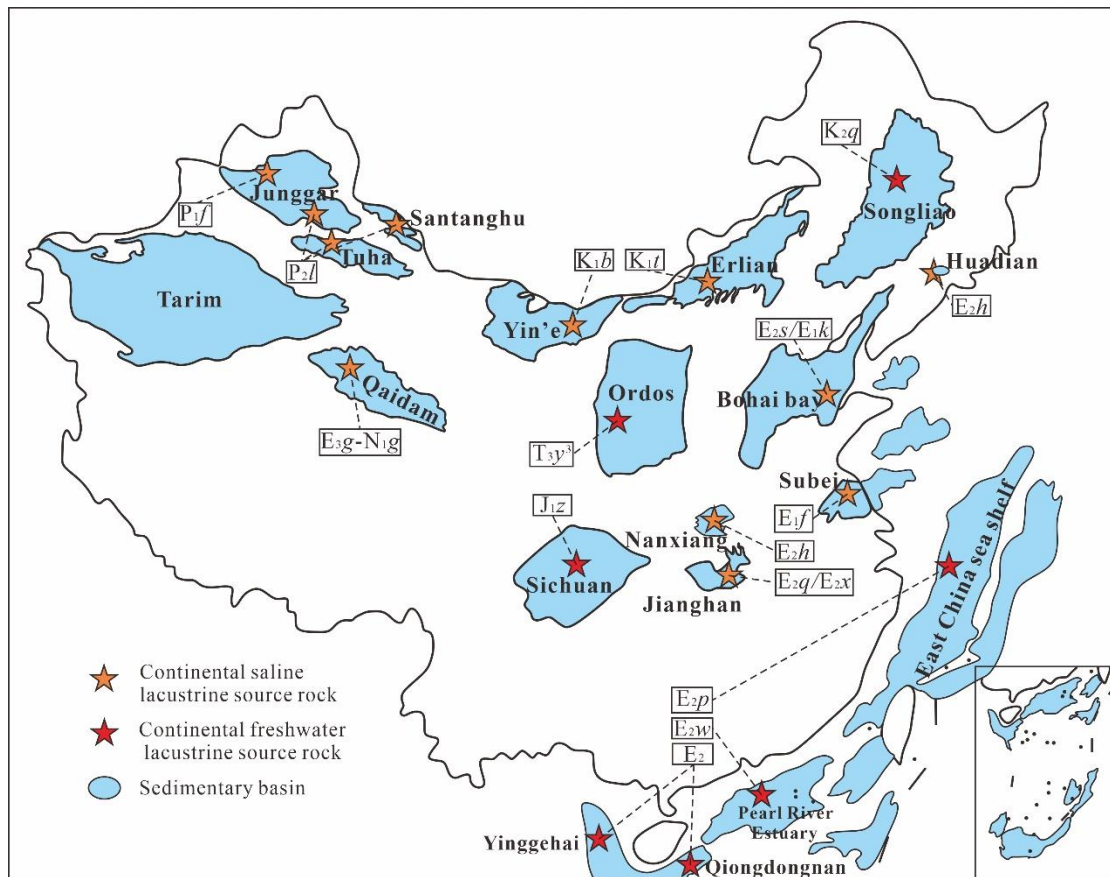


Figure 2 Spatial and temporal distribution of source rocks in continental lacustrine basins of China. Abbreviations: P, Permian; T, Triassic; J, Jurassic; K, Cretaceous; E, Eocene, N, Neogene.



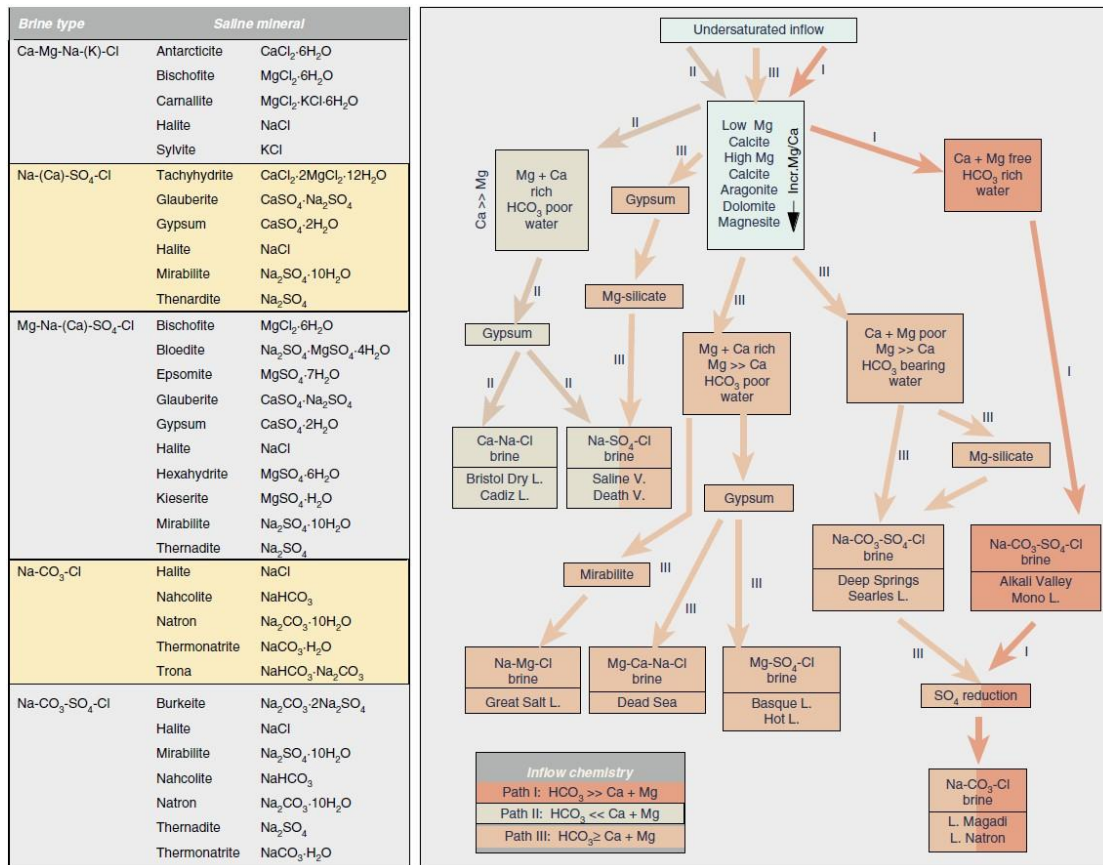


Figure 3 Hydrologic classification and brine evolution pathways of concentrating nonmarine waters and a listing of major evaporite minerals associated with the different brine types (from Warren, 2016)

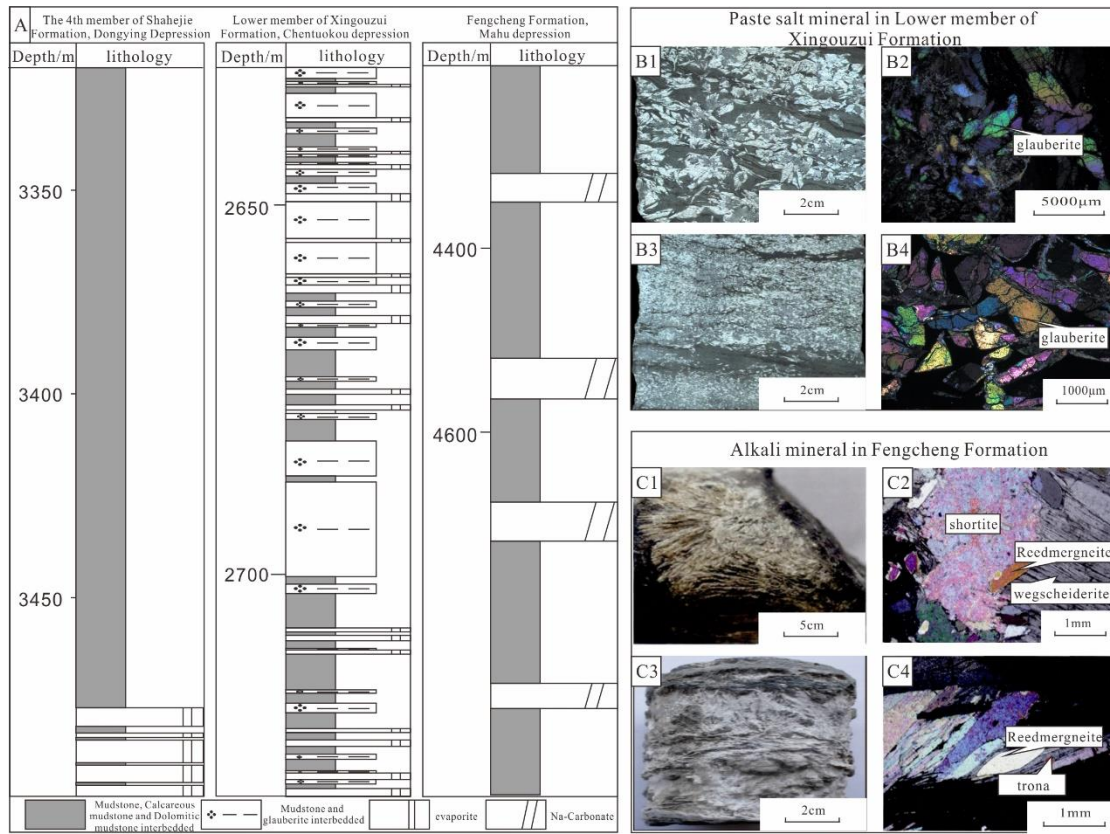


Figure 4 (A) Lithologic histogram of different types of saline lacustrine basins; (B1-B4) sulphate core and its microscopic characteristics; (C1-C4) Na carbonate cores and microscopic features (Figure C1-C4 from Wang et al., 2018; Cao et al., 2015)

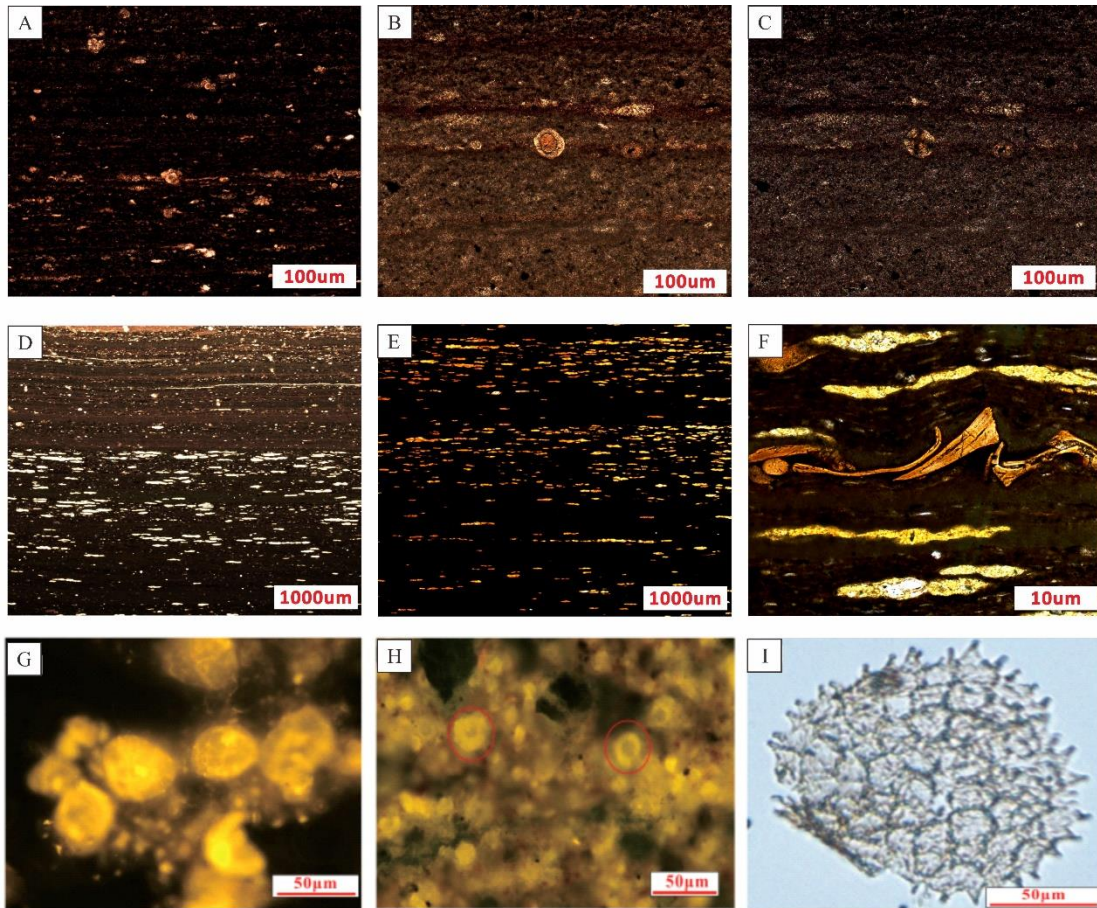


Figure 5 Characteristics of organic matter in shale of saline lacustrine basin. (A) Coccolithophores; (B) Coccolithophores; (C) Coccolithophores (cross extinction); (D) algal phytolites; (E) algal phytolites; (F) apatite

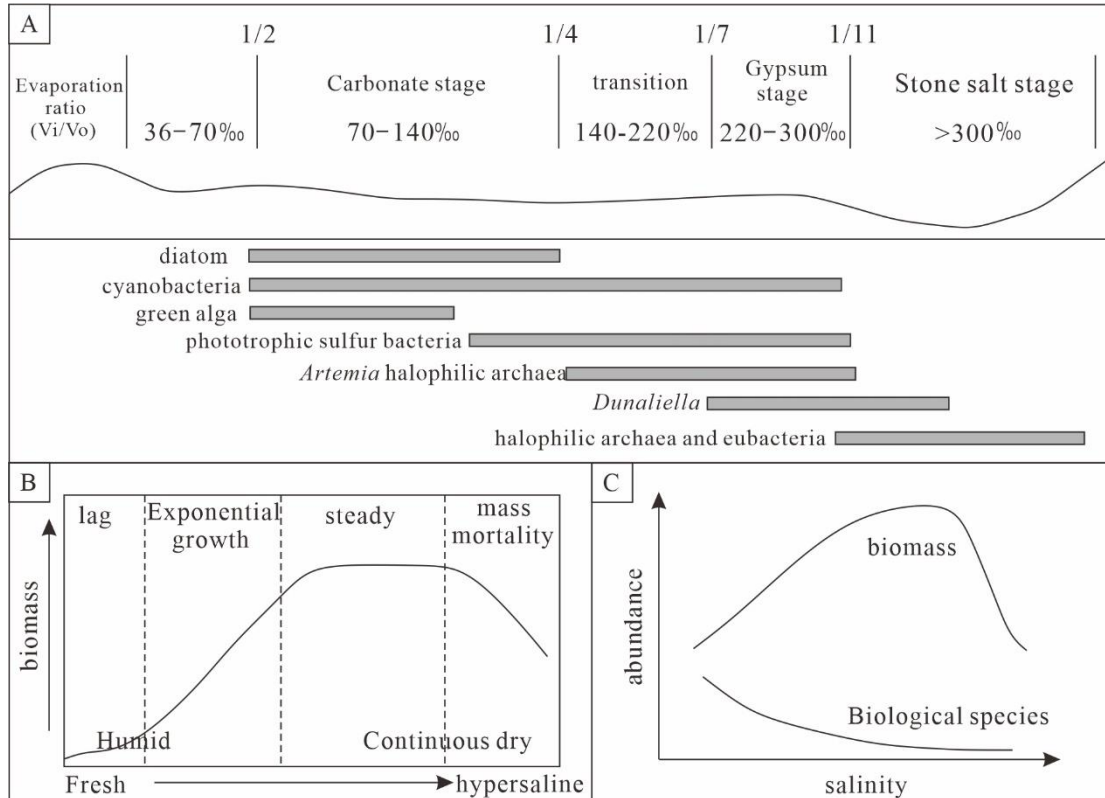


Figure 6 (A) Biological development of seawater with different salinities; (B) Mechanisms of biogenesis with salinity; (C) Relationship between species and biomass as salinity changes (Figure A modified from Barbe et al., 1990; Figure B and C modified from Warren, 2016)

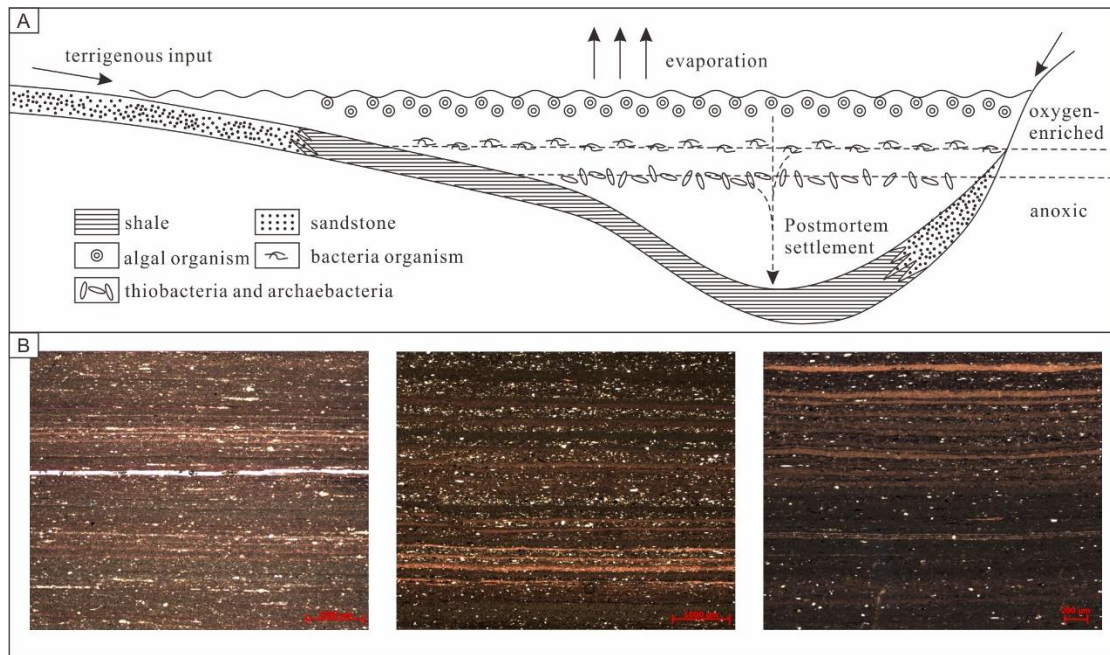


Figure 7 (A) Organic matter enrichment mechanism in stratified water; (B) Source rock laminar structure of saline lacustrine basin

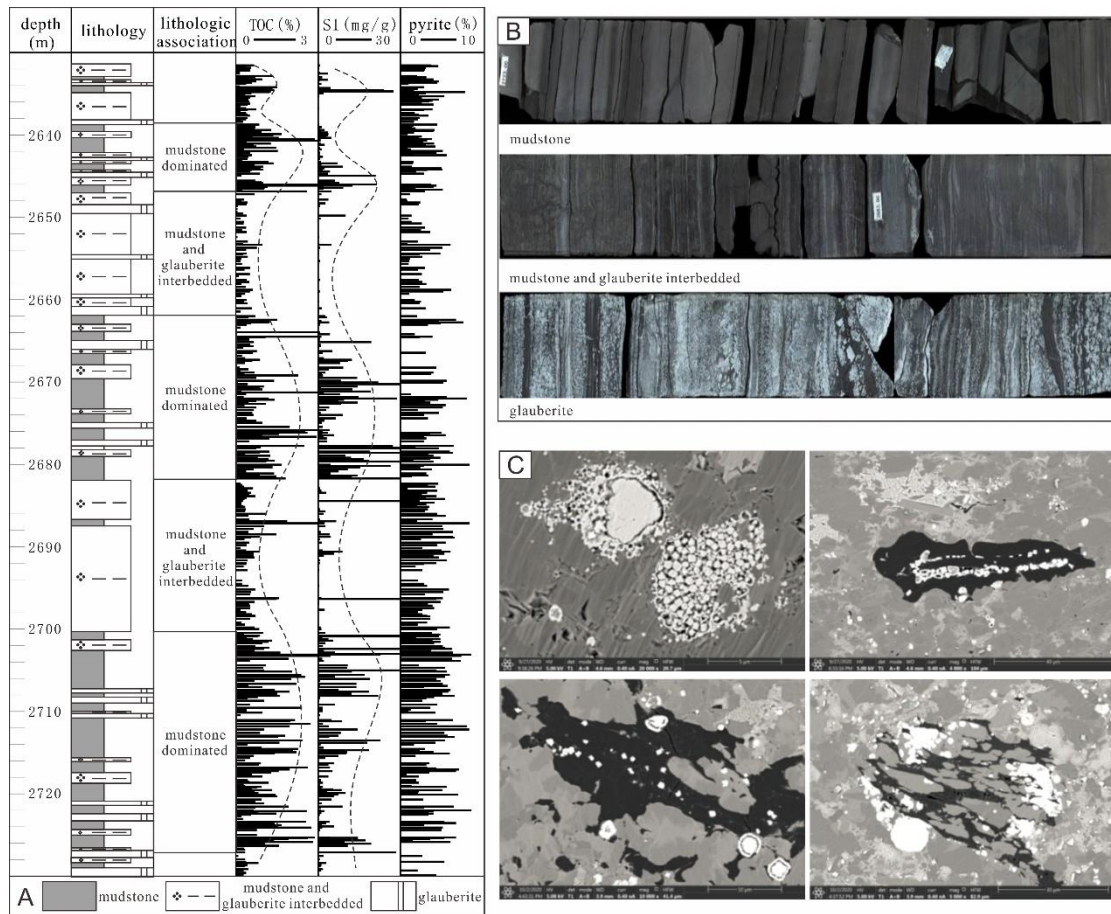


Figure 8 (A) Comprehensive histogram of the seventh Member of Dameigou Formation;

(B) Core photos of the seventh member of Dameigou Formation; (C) Pyrite

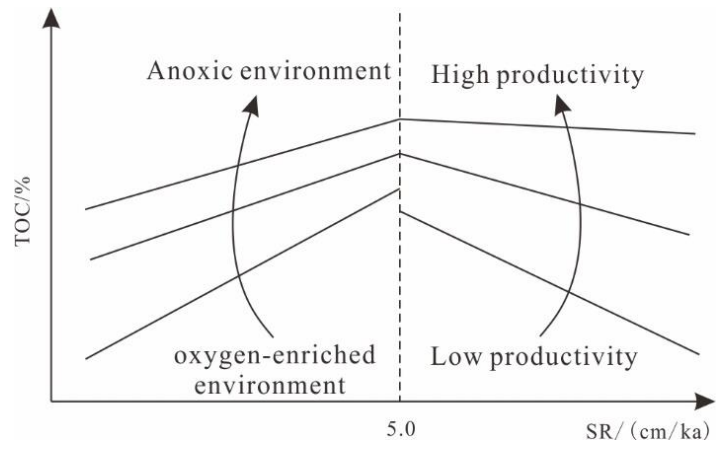


Figure 9 Relationship between deposition rate and organic carbon content (modified from Ding et al., 2015)

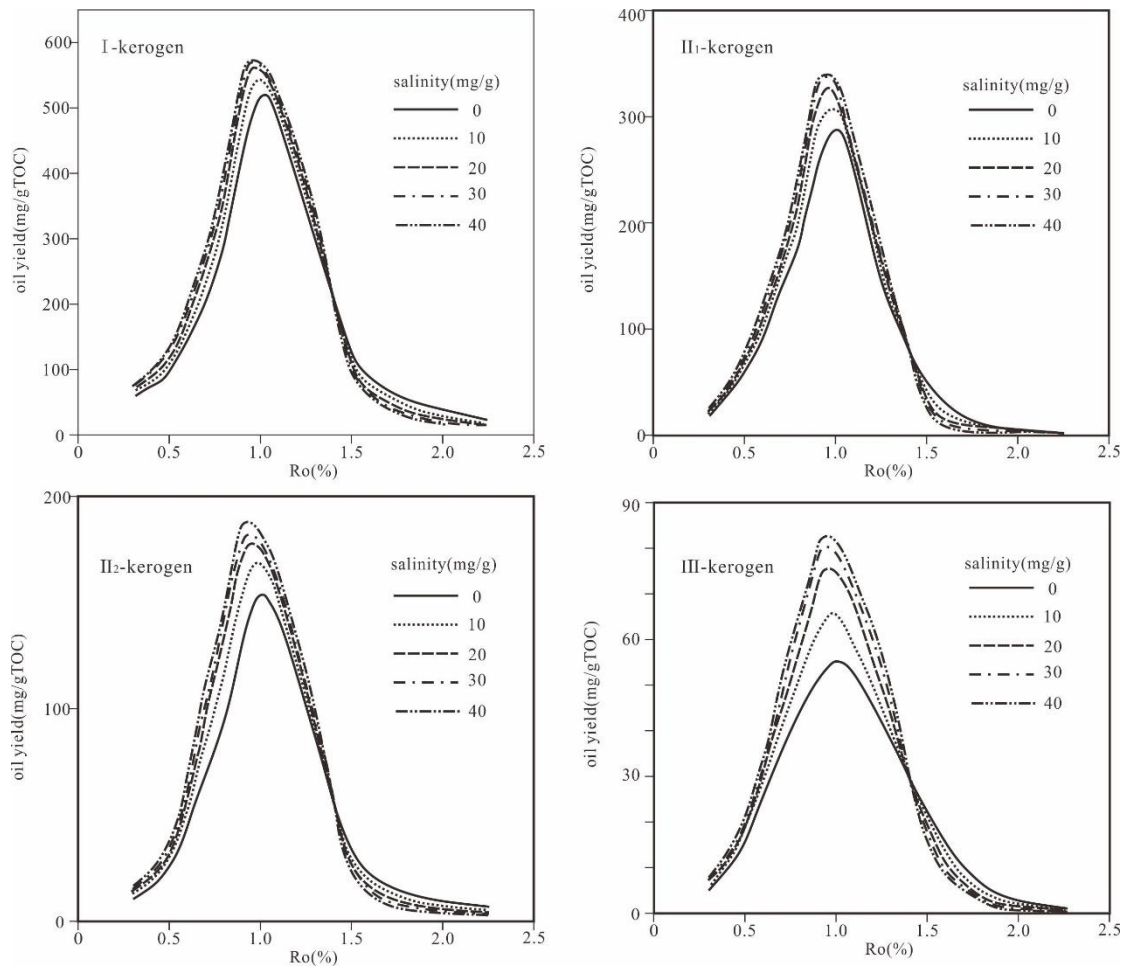


Figure 10 Effects of salts on hydrocarbon generation of different kerogens (modified from Ban, 2018)



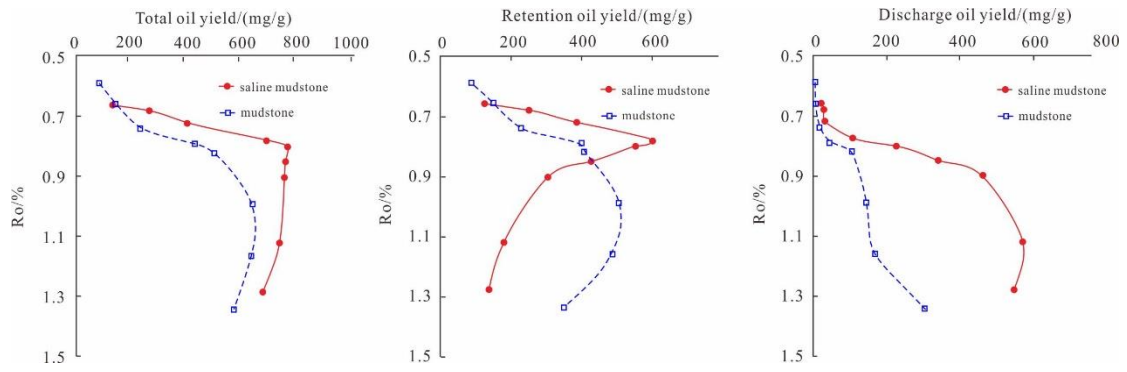


Figure 11 Simulation of hydrocarbon generation and expulsion from saline and non-saline shale samples (modified from Ma et al., 2013)

Table.1 Sedimentary rate of tertiary partially saline lacustrine basin (data from Jiang et al., 2004)

Basin	Qianjiang Depression Jiangnan Basin	Wuyang Depression Zhoukou Basin	Dongpu Depression Bohai Basin	Jinxian Depression Bohai bay Basin	Mangya Depression Qaidam Basin
stratigraphic	Eq	Eh	Es	Es <sub>4</sub> -E <sub>k</sub>	N <sub>1</sub> -E <sub>3</sub>
Maximum dep- osition thickness/m	4200	3800	>4000	>2000	4200
source rock thickness/m	2000	1400	2500	700	2500
deposition rate/ (cm/ka)	32	29	29	22	15